Available online at www.sciencedirect.com
SCIENCE DIRECT®
PERGAMON
Polyhedron 22 (2003) 3059–3064
POLYHEDRON
www.elsevier.com/locate/poly

Interface directed assembly of cyanide-bridged Fe–Co and Fe–Mn square grid networks

Jeffrey T. Culp [a], Ju-Hyun Park [b], Mark W. Meisel [b], Daniel R. Talham [a,*]

[a] Department of Chemistry, University of Florida, Gainesville, FL 32611-7200, USA
[b] Department of Physics and Center for Condensed Matter Sciences, University of Florida, Gainesville, FL 32611-8440, USA

Received 15 July 2002; accepted 27 August 2002

Abstract

Two isostructural square grid networks were formed by reacting a Langmuir monolayer of an amphiphilic pentacyanoferrate (3+) complex with aqueous Co^{2+} or Mn^{2+} ions dissolved in the subphase. Confinement of the reactants to the air–water interface discriminates against the formation of higher dimensional products and directs the lateral propagation of a polymeric two-dimensional cyanide-bridged network. The network can be transferred to a variety of supports to form monolayer or multilayer lamellar films by the Langmuir–Blodgett (LB) technique. Characterization of both the Fe–Co and Fe–Mn LB film extended networks by FTIR spectroscopy, SQUID magnetometry, and grazing incidence synchrotron X-ray diffraction (GIXD) reveals face-centered square grid structures directed by the defined bond angles of the octahedral metal complexes and the linear cyanide bridges. Magnetic measurements on both samples indicate the presence of anisotropic low temperature magnetic exchange interactions between the paramagnetic centers. The results illustrate the potential utility of an interface as a structure director in the assembly of low dimensional coordinate covalent network solids.

Keywords: Magnetic thin films; Metal cyanide square grid; Langmuir–Blodgett; GIXD

1. Introduction

Coordination chemistry routes to finite and infinite networks make use of the predictable directional characteristics of coordinate covalent bonds [1–9]. Tunable variables like stoichiometry, template additives, secondary structure building blocks, or kinetic control are used to determine the final network structure, and several examples are included in the current issue. Potential applications of inorganic finite and infinite networks include recognition and sensing, catalysis, electronic and optical functions, and magnetic effects related to information storage [1,10,11]. It is interesting to note that several of these applications are likely to involve positioning at surfaces, and routes to locate the finite or infinite networks at interfaces will be needed [12–22]. One approach is to involve the interface directly in the assembly, to carry out the network fabrication where it will be located. In this case, the interface can play a role in determining the network structure. Examples of assembly at liquid interfaces have been published, including some two-dimensional infinite networks [19,20,23–27]. The surface of a liquid retains the structure directing character of an interface, but at the same time is fluidic and can facilitate diffusion of reactants. Careful understanding of these processes is now possible largely as a result of surface sensitive characterization methods, including grazing incidence X-ray diffraction as detailed in a recent review [27].

We recently reported the fabrication of an Fe^{3+}/Ni^{2+} mixed-metal cyanide-bridged square grid network at the air–water interface, showing that the interface can act as a structure directing entity when preparing coordinate covalent networks [28]. In this paper, we show the process is general and describe two new examples of square grid networks prepared as monolayers at the air–water interface. The technique, outlined in Scheme 1, uses the air–water interface and involves the reaction of

* Corresponding author. Tel.: +1-352-392-9016; fax: +1-352-392-3255.
E-mail address: talham@chem.ufl.edu (D.R. Talham).

0277-5387/$ - see front matter © 2003 Elsevier Ltd. All rights reserved.
doi:10.1016/S0277-5387(03)00425-X

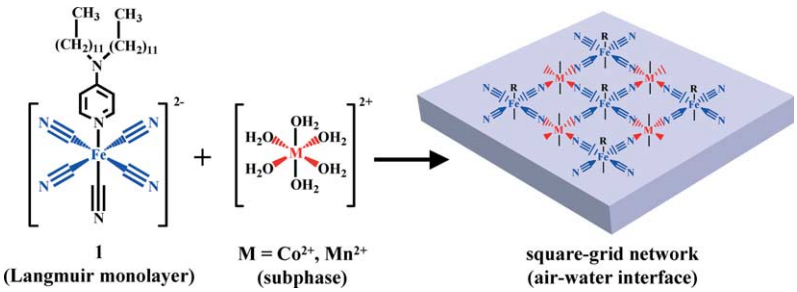

Scheme 1. Assembly of two-dimensional grid networks at the air–water interface.

an amphiphilic pentacyanoferrate (3+) complex **1** confined to a monolayer on a aqueous subphase containing a second divalent metal ion. By confining one of the reactants to the air–water interface the propagation of the structure in the third dimension is prevented, resulting in a planar network at the water surface. The effect of the interface works in tandem with the defined bond angles of the octahedral metal complexes and the linear geometry of the cyanide bridge to direct the final structure of the network to a face-centered square grid array. The same reactants in a homogeneous reaction give amorphous colloidal products, thus illustrating the ability of an interface to direct the structure of the network. Also, the interface-assembled network can be conveniently transferred to solid supports by the Langmuir–Blodgett technique, permitting added structural and material property characterization.

The cyanide ligand is particularly attractive for use in network assembly. Its linear geometry and ambidentate nature make for a versatile building block when combined with various transition metal complex geometries [29–40]. In addition, cyanide has been shown to mediate both magnetic and electronic exchange between the bridged metal centers, giving rise to materials with interesting physical properties, including a family of molecule-based magnets [29–32,41–43]. We previously reported an Fe^{3+}/Ni^{2+} cyanide bridged network prepared at the air–water interface and showed it to be magnetic [28]. This study extends the series to include Fe^{3+}/Co^{2+} and Fe^{3+}/Mn^{2+} mixed metal cyanide networks. These new two-dimensional networks are also magnetic, and their behavior is compared to those of related three-dimensional hexacyanometallate complexes.

2. Experimental

2.1. Materials

The amphiphilic complex tetramethylammonium pentacyano(4-didodecylaminopyridine)ferrate(III) $\cdot 6H_20$ was prepared as previously described [28]. Attenuated total reflectance (ATR) FT-IR samples were prepared as monolayers on clean silicon ATR crystals. Grazing incidence X-ray diffraction (GIXD) samples were prepared on petrographic slides that were first cleaned using the RCA procedure [44] and made hydrophobic by deposition of a monolayer of octadecyltrichlorosilane [45,46]. Samples for SQUID magnetometry measurements were prepared on Mylar (Dupont) substrates cleaned with absolute ethanol prior to use.

2.2. Film preparation

The amphiphilic iron complex **1** was spread onto the water surface from a chloroform solution. Multilayer films of the iron–cyanide–manganese and iron–cyanide–cobalt networks were transferred as Y-type films onto hydrophobic substrates at a surface pressure of 25 mN/m over a subphase 1 g/l in $Mn(NO_3)_2 \cdot xH_2O$ or $Co(NO_3)_2 \cdot xH_2O$ at ambient temperature. Transfer ratios for both the upstrokes and downstrokes were between 0.85 and 1.0 for all layers.

2.3. Instrumentation

IR spectra were collected using a Mattson Instruments (Madison, WI) Research Series-1 FTIR spectrometer with a deuterated triglycine sulfate (DTGS) detector. The LB films were prepared by using a KSV Instrument 5000 through modified to operate with double barriers. The surface pressure was measured with a filter paper Wilhelmy plate suspended from a KSV microbalance. Subphase solutions were prepared from 17.8 to 18.1 MΩ cm water delivered with a Barnstead Epure system. Magnetization measurements were performed on a Quantum Design MPMS SQUID magnetometer. GIXD experiments using synchrotron radiation were performed at the Advanced Photon Source, Argonne, IL, at the Materials Research Collaborative Access Team beamline (sector 10) [28,47]. The GIXD scans were performed on LB films transferred to glass slides. The sample was positioned in the center of an 8-circle Huber goniometer and oriented at an angle of 0.13° relative to the incident beam. The incident beam was collimated to 200 μm high by 1500 μm

wide and tuned to a wavelength of 1.254 Å. Diffracted intensity in the *xy* plane was measured using a NaI scintillation counter mounted on the Huber goniometer. The diffracted signal was collimated prior to the detector using Soller slits giving an experimental resolution of the order of 0.015 $Å^{-1}$.

3. Results and discussion

3.1. Langmuir monolayers

Evidence for the condensation reaction is first seen directly at the air–water interface using the traditional Langmuir monolayer methods of Brewster angle microscopy (BAM) and pressure vs area isotherms. At room temperature, the amphiphilic pentacyanoferrate (3+) complex **1** is in a liquid expanded phase on water (with 10^{-3} M NaCl). The BAM image in Fig. 1(a) shows a two-dimensional foam of the liquid expanded phase that forms upon spreading. As the film is compressed, a continuous film forms. The pressure vs area isotherm for **1** does not show evidence for a phase transition with increased pressure, indicating that **1** maintains the liquid expanded phase up until collapse.

If a complexing metal ion (Mn^{2+} or Co^{2+}) is added to the subphase, the amphiphile behaves very differently, forming a condensed phase at all pressures. The monolayer must be compressed to a much smaller area before the surface pressure increases (Fig. 2). After the surface pressure begins to rise, the slope is much sharper than in the absence of complexing ions, reflecting the lower compressibility of the film. The condensed phase over Mn^{2+} is seen in the BAM image, Fig. 1(b). The behavior is consistent with crosslinking of the amphiphiles by the subphase metal ions through cyanide bridges to form a network.

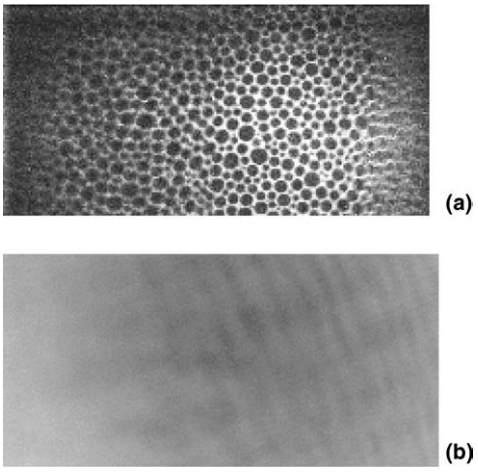

Fig. 1. BAM images taken at zero surface pressure of complex **1** over (a) 10^{-3} M NaCl and (b) 1 g/l $Mn(NO_3)_2$ subphase.

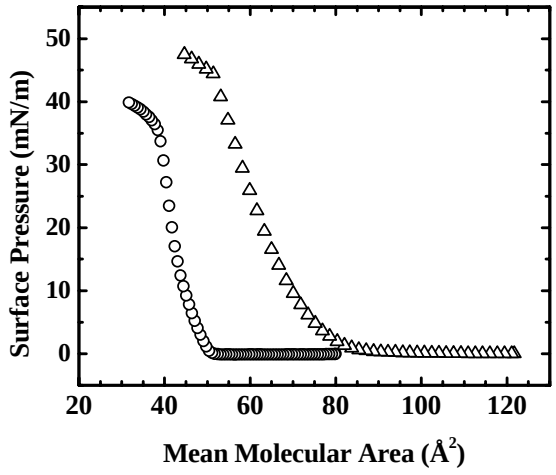

Fig. 2. Room temperature surface pressure vs mean molecular area isotherms for complex **1** over pure water (△) and 1g/l $Co(NO_3)_2$ (○).

3.2. Tansferred films

3.2.1. Infrared spectroscopy

The network monolayers can be transferred onto solid supports using traditional LB deposition procedures, permitting further structural and physical property characterization. Evidence for cyanide bridging is seen by FTIR. Attenuated total reflectance FTIR spectra of the cyanide stretches for the condensed films are compared in Fig. 3 to those of **1**, obtained as a KBr pellet. The spectrum of complex **1** shows a band at 2111 cm^{-1} with a shoulder at 2128 cm^{-1} and is in the typical range with the expected splitting for an Fe^{3+} pentacyanide complex. The Fe–Mn film shows a broad band centered at 2145 cm^{-1} and agrees well with the CN stretching frequency reported for the related $Mn_3[Fe(CN)_6]$ Prussian blue analog [48], confirming the presence of Fe–CN–Mn bridging in the film. The FTIR spectrum for

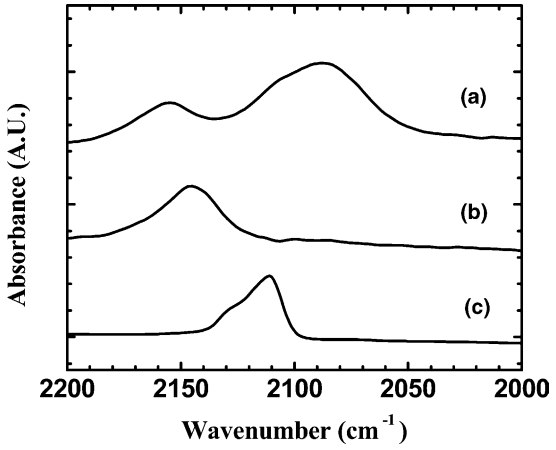

Fig. 3. Infrared absorbance spectra of the C–N stretching region for monolayer films on Si ATR crystals of the grid network formed from the reaction of complex **1** with (a) Co^{2+} and (b) Mn^{2+} compared to (c) the spectrum of **1** as a KBr pellet.

the Fe–Co film is more complex and shows a split band with a peak at 2155 cm^{-1} and a broad peak at 2090 cm^{-1}. A similar splitting has been reported in a $Co[Fe(CN)_6]$ Prussian blue analog and has been attributed to the presence of two different oxidation states of the iron cyanide complex [49]. The peak at higher wavenumbers is due to an Fe^{3+}–CN–Co^{2+} bridge and the lower energy peak to an Fe^{2+}–CN–Co^{2+} bridge. The band reported at 2133 cm^{-1} for $Co[Fe(CN)_6]$ attributed to an Fe^{2+}–CN–Co^{3+} bridge is not observed in the monolayer Fe–Co film. The IR data suggest that some Fe^{3+} is reduced in the network, as in the three-dimensional analog, but the relatively large excess of Co^{2+} in the subphase assures that any Co^{3+} that forms in the network is quickly reduced, leaving only Co^{2+} in the film.

3.2.2. Grazing incidence X-ray diffraction

The in-plane structure of the networks is confirmed by X-ray diffraction. The small quantity of material and strong background scattering make conventional X-ray sources ineffective for characterizing the in-plane structure of thin films. However, the combination of enhanced X-ray flux from synchrotron radiation with grazing incidence angles reduces the signal-to-noise ratio to a level where scattering from as little as a monolayer film can be detected. This method of grazing incidence X-ray diffraction (GIXD) has been described in detail [50]. The GIXD patterns obtained on 15-bilayer samples of the Fe–Mn and Fe–Co networks transferred to glass slides are shown in Fig. 4. Both patterns show the same three peaks, with slight shifts in spacing, and confirm that the Fe–Mn and Fe–Co networks are isostructural. The diffraction peaks for the Fe–Mn film correspond to lattice spacings of 5.18, 3.69, and 2.61 Å. The analogous spacings for the Fe–Co film are 5.10, 3.62, and 2.55 Å, respectively. Both patterns can be indexed to a face-centered square network with Miller indices of (20), (22), and (40), in the order from large to small spacings, and yield face-centered square unit cells of $a = 10.36$ Å for the Fe–Mn and $a = 10.20$ Å for the Fe–Co networks. Analysis of the peak widths of the (20) and (40) reflections in both films by application of the Scherrer equation [51] yields a structural coherence length of approximately 80 Å for both films.

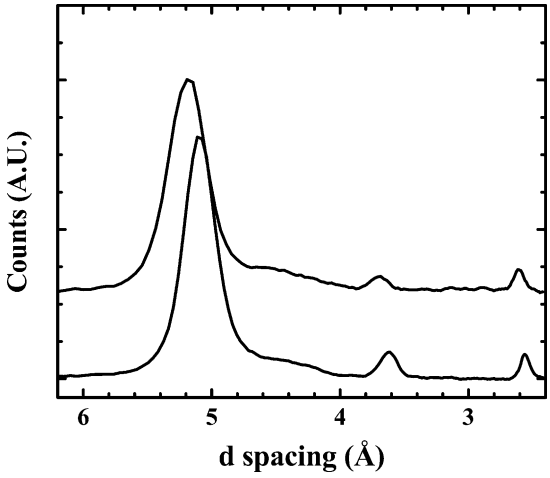

Fig. 4. Grazing incidence X-ray diffraction patterns for 10 bilayer samples on glass of the (a) Fe–Mn and (b) Fe–Co grid networks. Each pattern can be indexed to a face-centered square grid network with cell edges of 10.36 and 10.20 Å, respectively.

3.2.3. Magnetism

The three-dimensional analogs $Mn_3[Fe(CN)_6]_2$ and $Co_3[Fe(CN)_6]_2$ are low-temperature ferrimagnets with T_c of 9 and 14 K, respectively [52]. Magnetic exchange in these compounds is mediated by the cyanide ligand. The temperature dependent magnetization for the two-dimensional assemblies is reported in Fig. 5 for the Fe–Co film and in Fig. 6 for the Fe–Mn film, each in two

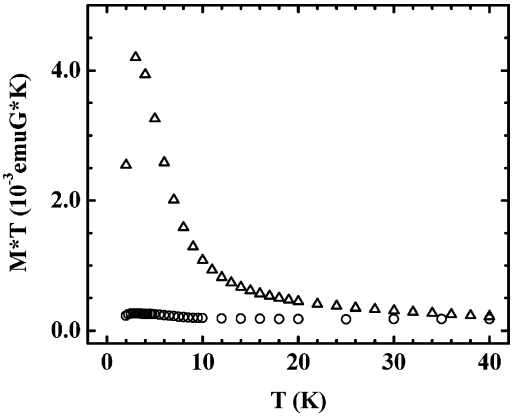

Fig. 5. The temperature dependence of the product of the zero-field cooled magnetization (measured in 20 G) and temperature for a 100 bilayer (per side) sample of the Fe–Co network on Mylar showing the anisotropy of the magnetic response when the field is applied parallel to the sample surface (△) and perpendicular to the sample surface (○).

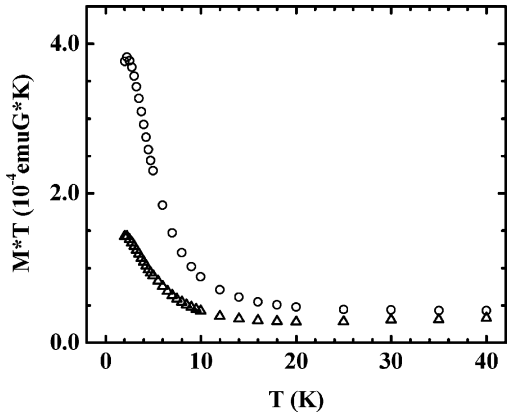

Fig. 6. The temperature dependence of the product of the zero-field cooled magnetization (measured in 20 G) and temperature for a 125 bilayer (per side) sample of the Fe–Mn network on Mylar showing the anisotropy of the magnetic response when the field is applied perpendicular to the sample surface (○) and parallel to the sample surface (△).

orientations. The Fe–Co sample was 100 bilayers per side and the Fe–Mn sample 125 bilayers per side. Both films were on 10 cm^2 of Mylar substrate. The magnetic behavior of each film is consistent with the ferrimagnetic exchange observed for the three-dimensional parent compounds, although a significant diamagnetic background contribution from the Mylar substrate makes it difficult to unambiguously quantify the moments to discern ferrimagnetism from ferromagnetic exchange in the transferred films.

The magnetic response of each film is anisotropic with respect to the sample orientation in the applied magnetic field. The Fe–Co film shows negligible magnetic response (Fig. 5) when the field is applied perpendicular to the magnetic planes. Conversely, magnetization increases rapidly below 10 K with the applied field parallel to the plane of the network. The magnetic response of the Fe–Mn film (Fig. 6) is also anisotropic, but in the opposite sense. The variation in the orientation of the magnetic easy axes must reflect the reduced symmetries of the crystal fields in the two-dimensional networks and the differences in single ion anisotropies expected for Co^{2+}, Mn^{2+}, and low spin Fe^{3+}. The pentacyanoferrate (3+) complex common to both structures is a low-spin d^5 ion, known to experience significant spin–orbit coupling [53]. In addition, the 4-aminopyridine ligand and bridging of the in-plane cyanides lower the symmetry of the Fe^{3+} site. When coupled with the isotropic $S = 5/2$ Mn^{2+} ion, the ferric site can be expected to define the magnetic easy axis. In the case of the Fe–Co material, the strong Ising character of the Co^{2+} ion dominates, in this case confining the moments to the network plane. The anisotropy of the Fe–Co film is similar to that observed for the analogous Fe–Ni film that was described previously [28].

When the monolayers are transferred to solid supports for magnetic studies they form bilayers with the metal cyanide networks depositing face-to-face. Each inorganic bilayer is then separated from the next by the alkyl tails of the amphiphilic aminopyridine ligand. The exact nature of the interaction between the face-to-face networks is not yet clear nor is its influence on the anisotropic response. More detailed magnetic studies comparing true monolayers with the multilayer films are underway. Nevertheless, magnetic exchange in the films provides additional evidence that extended networks form in the condensation reaction at the air–water interface. In addition, the anisotropic magnetic behavior discriminates against a cubic Prussian blue-like product and is consistent with a planar structure.

4. Conclusions

Reaction of an amphiphilic pentacyanoferrate (3+) complex at the air–water interface with divalent metal ions from the subphase results in two-dimensional cyanide-bridged coordinate-covalent networks. Confining one of the reactants to the surface of water illustrates the concept that the interface can be used as a structure-directing element for preparing two-dimensional arrays. The same reaction in the absence of the interface generates amorphous colloids. The cyanide bridges mediate magnetic exchange, just as in the related three-dimensional hexacyanometallate analogs, but the two-dimensional networks lead to anisotropic behavior that changes with the identity of the metal ions.

Acknowledgements

The authors would like to thank Dr. Christophe Mingotaud for his assistance with the BAM images. This research was supported by the National Science Foundation through Grant DMR-9900855 (DRT) and by the American Chemical Society through Grant ACS-PRF-36163-AC5 (MWM, DRT). Use of the Advanced Photon Source was supported by the US Department of Energy, Office of Science, Office of Basic Energy Sciences, under Contract No. W-31-109-ENG-38. We also acknowledge support from the Materials Research Collaborative Access Team (MRCAT) at the Advanced Photon Source.

References

[1] J.M. Lehn, Angew. Chem., Int. Ed. Engl. 29 (1990) 1304.
[2] P.J. Stang, B. Olenyuk, Acc. Chem. Res. 30 (1997) 502.
[3] A.J. Blake, N.R. Champness, P. Hubberstey, W.S. Li, M.A. Withersby, M. Schroder, Coord. Chem. Rev. 183 (1999) 117.
[4] G.F. Swiegers, T.J. Malefetse, Chem. Rev. 100 (2000) 3483.
[5] P.J. Stang, Chem. Eur. J. 4 (1998) 19.
[6] B. Olenyuk, J.A. Whiteford, A. Fechtenkotter, P.J. Stang, Nature 398 (1999) 796.
[7] S.R. Batten, R. Robson, Angew. Chem., Int. Ed. Engl. 37 (1998) 1461.
[8] M. Fujita, K. Ogura, Coord. Chem. Rev. 148 (1996) 249.
[9] M. Fujita, S.Y. Yu, T. Kusukawa, H. Funaki, K. Ogura, K. Yamaguchi, Angew. Chem., Int. Ed. Engl. 37 (1998) 2082.
[10] P.H. Dinolfo, J.T. Hupp, Chem. Mater. 13 (2001) 3113.
[11] A.M. Morales, C. Lieber, Science 279 (1998) 208.
[12] U. Ziener, J.-M. Lehn, A. Mourran, M. Moller, Chem. Eur. J. 8 (2002) 951.
[13] A. Semenov, J.P. Spatz, M. Moller, J.-M. Lehn, B. Sell, D. Schubert, C.H. Weidl, U.S. Schubert, Angew. Chem., Int. Ed. Engl. 38 (1999) 2547.
[14] A. Shipway, I. Willner, Acc. Chem. Res. 34 (2001) 421.
[15] F. Armand, P. Albouy, F. Cruz, M. Normand, V. Huc, E. Goron, Langmuir 17 (2001) 3431.
[16] N. Bowden, A. Terfort, J. Carbeck, G.M. Whitesides, Science 276 (1997) 233.
[17] N. Bowden, I.S. Choi, B.A. Grzybowski, G.M. Whitesides, J. Am. Chem. Soc. 121 (1999) 5375.
[18] N. Bowden, F. Arias, T. Deng, G.M. Whitesides, Langmuir 17 (2001) 1757.

[19] I. Weissbuch, P.N.W. Baxter, S. Cohen, H. Cohen, K.K. Jaer, P.B. Howes, J. Als-Nielsen, G.S. Hanan, U.S. Schubert, J.-M. Lehn, L. Leiserowitz, M. Lahav, J. Am. Chem. Soc. 120 (1998) 4850.
[20] I. Weissbuch, P.N.W. Baxter, I. Kuzmenko, H. Cohen, S. Cohen, K. Kjaer, P.B. Howes, J. Als-Nielsen, J.-M. Lehn, L. Leiserowitz, M. Lahav, Chem. Eur. J. 6 (2000) 725.
[21] C. Mingotaud, C. Lafuente, J. Amiell, P. Delhaes, Langmuir 15 (1999) 289.
[22] Q. Huo, K.C. Russell, R.M. LeBlanc, Langmuir 14 (1998) 2174.
[23] T.F. Magnera, J. Pecka, J. Vacek, J. Michl, Nanostructured Materials, American Chemical Society, Washington, DC, 1997, p. 213.
[24] T.F. Magnera, L.M. Peslherbe, E. Korblova, J. Michl, J. Organomet. Chem. 548 (1997) 83.
[25] J. Michl, T.F. Magnera, Proc. Natl. Acad. Sci. USA 99 (2002) 4788.
[26] N. Varaksa, L. Pospíil, T.F. Magnera, J. Michl, Proc. Natl. Acad. Sci. USA 99 (2002) 5012.
[27] I. Kuzmenko, H. Rapaport, K. Kjaer, J. Als-Nielsen, I. Weissbuch, M. Lahav, L. Leiserowitz, Chem. Rev. 101 (2001) 1659.
[28] J.T. Culp, J.-H. Park, D. Stratakis, M.W. Meisel, D.R. Talham, J. Am. Chem. Soc. 124 (2002) 10083.
[29] V. Gadet, T. Mallah, I. Castro, M. Verdaguer, J. Am. Chem. Soc. 114 (1992) 9213.
[30] T. Mallah, S. Thiebaut, M. Verdaguer, P. Veillet, Science 262 (1993) 1554.
[31] S. Ferlay, T. Mallah, R. Ouahes, P. Veillet, M. Verdaguer, Nature 378 (1995) 701.
[32] M. Ohba, N. Fukita, H. Okawa, J. Chem. Soc., Dalton Trans. 10 (1997) 1733.
[33] N. Re, E. Gallo, C. Floriani, H. Miyasaka, N. Matsumoto, Inorg. Chem. 35 (1996) 6004.
[34] H. Miyasaka, N. Matsumoto, H. Kawa, N. Re, E. Gallo, C. Floriani, J. Am. Chem. Soc. 118 (1996) 981.
[35] M. Ohba, H. Okawa, N. Fukita, Y. Hashimoto, J. Am. Chem. Soc. 119 (1997) 1011.
[36] Z.J. Zhong, H. Seino, Y. Mizobe, M. Hidai, A. Fujishima, S. Ohkoshi, K. Hashimoto, J. Am. Chem. Soc. 122 (2000) 2952.
[37] P.A. Berseth, J.J. Sokol, M.P. Shores, J.L. Heinrich, J.R. Long, J. Am. Chem. Soc. 122 (2000) 9655.
[38] J. Larionova, M. Gross, M. Pilkington, H. Andres, H. Stoeckli-Evans, H.U. Gudel, S. Decurtins, Angew. Chem., Int. Ed. Engl. 39 (2000) 1605.
[39] K.R. Dunbar, R.A. Heintz, Prog. Inorg. Chem. 45 (1997) 283.
[40] G. Rogez, S. Parsons, C. Paulsen, V. Villar, T. Mallah, Inorg. Chem. 40 (2001) 3836.
[41] O. Hatlevik, W.E. Buschmann, J. Zhang, J.L. Manson, J.S. Miller, Adv. Mater. 11 (1999) 914.
[42] S.M. Holmes, G.S. Girolami, J. Am. Chem. Soc. 121 (1999) 5593.
[43] W.R. Entley, G.S. Girolami, Science 268 (1995) 397.
[44] W. Kern, J. Electrochem. Soc. 137 (1990) 1887.
[45] R. Maoz, J. Sagiv, J. Coll. Interface Sci. 100 (1984) 465.
[46] L. Netzer, J. Sagiv, J. Am. Chem. Soc. 105 (1983) 674.
[47] See http://ixs.csrri.iit.edu/mrcat/ for additional information.
[48] J.F. Bertrán, J.B. Pascual, M. Hernández, R. Rodríguez, React. Solids 5 (1988) 95.
[49] O. Sato, Y. Einaga, A. Fujishima, K. Hashimoto, Inorg. Chem. 38 (1999) 4405.
[50] J. Als-Nielsen, D. Jacquemain, K. Kjaer, F. Leveiller, M. Lahav, L. Leiserowitz, Phys. Rep. 246 (1994) 251.
[51] A. Guinier, X-ray Diffraction, Freeman, San Francisco, 1968.
[52] V. Gadet, M. Bujoli-Doeuff, L. Force, M. Verdaguer, E. Makhi, A. Deroy, J.P. Besse, C. Chappert, P. Veillet, J.P. Renard, P. Beauvillain, in: J.D. Gatteschi, O. Kahn, J.S. Miller, F. Palacio (Eds.), Molecular Magnetic Materials, NATO ASI Series, Series E, vol. 198, Kluwer Academic Publishers, Dordrecht, 1991, p. 281.
[53] R.L. Carlin, Magnetochemistry, Springer, Berlin/Heidelberg, 1986.